

AD-A017 321

AIRFOIL PROFILE DRAG

Milton A. Schwartzberg

Army Aviation Systems Command
St. Louis, Missouri

June 1975

DISTRIBUTED BY:

NTIS

National Technical Information Service
U. S. DEPARTMENT OF COMMERCE

325070

AD

USAAVSCOM TECHNICAL REPORT 75-19

AIRFOIL PROFILE DRAG

Systems Research Integration Office

June 1975

APPROVED FOR PUBLIC RELEASE;
DISTRIBUTION UNLIMITED.

U.S. ARMY AVIATION SYSTEMS COMMAND

St. Louis, Mo. 63102

**U.S. ARMY AIR MOBILITY RESEARCH AND
DEVELOPMENT LABORATORY**

Moffett Field, Ca. 94035

D D C
RECEIVED
NOV 18 1975
RECEIVED
D



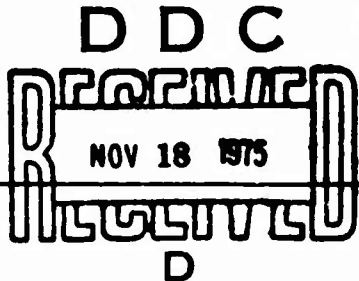
Reproduced by
**NATIONAL TECHNICAL
INFORMATION SERVICE**
U S Department of Commerce
Springfield VA 22151

AD A 0 1 7 3 2 1

ADDITION BY		
DTG	With Section	<input checked="" type="checkbox"/>
DCS	Not Section	<input type="checkbox"/>
UNANNOUNCED		<input type="checkbox"/>
JUSTIFICATION		
BY		
DISTRIBUTION/AVAILABILITY GROUP		
Dist.	AVAIL. MOD/W	SPECIAL
A		

DISCLAIMER STATEMENT

The findings in this report are not to be construed as
an official Department of the Army position.

REPORT DOCUMENTATION PAGE		READ INSTRUCTIONS BEFORE COMPLETING FORM
1. REPORT NUMBER USAAVSCOM Technical Report 75-19	2. GOVT ACCESSION NO.	3. RECIPIENT'S CATALOG NUMBER
4. TITLE (and Subtitle) Airfoil Profile Drag		5. TYPE OF REPORT & PERIOD COVERED Final
7. AUTHOR(s) Milton A. Schwartzberg		6. PERFORMING ORG. REPORT NUMBER
9. PERFORMING ORGANIZATION NAME AND ADDRESS Systems Research Integration Office (SAVDL-SR) St. Louis, Missouri 63102		8. CONTRACT OR GRANT NUMBER(s)
11. CONTROLLING OFFICE NAME AND ADDRESS US Army Aviation Systems Command St. Louis, Missouri 63102		10. PROGRAM ELEMENT, PROJECT, TASK AREA & WORK UNIT NUMBERS 1F262209AH76
14. MONITORING AGENCY NAME & ADDRESS (if different from Controlling Office) US Army Air Mobility Research and Development Laboratory Moffett Field, California 94035		12. REPORT DATE June 1975
		13. NUMBER OF PAGES 38
		15. SECURITY CLASS. (of this report) Unclassified
16. DISTRIBUTION STATEMENT (of this Report) Distribution of this document is unlimited		15a. DECLASSIFICATION/DOWNGRADING SCHEDULE
17. DISTRIBUTION STATEMENT (of the abstract entered in Block 20, if different from Report)		
18. SUPPLEMENTARY NOTES		
19. KEY WORDS (Continue on reverse side if necessary and identify by block number) Drag, Profile Drag, Airfoil Drag, Profile Power		
20. ABSTRACT (Continue on reverse side if necessary and identify by block number) A method is presented for the estimation of the profile drag coefficient of airfoils at subsonic Mach numbers below the drag rise values. The method is applicable to smooth airfoils, with fully turbulent boundary layers, at any Reynolds number. The method is simple to apply for rapid estimation purposes, and to incorporate into an aircraft performance computation procedure.		

INTRODUCTION

The present study was prompted by a need for a reasonably accurate helicopter performance prediction method, simple enough to program on a desk-top size computer. Such a program is intended for preliminary design work and design evaluations.

The problem area covered in this paper is that of the estimation of airfoil (two-dimensional) profile drag. The treatment is confined to the consideration of smooth airfoils with fully turbulent boundary layers. Such an airfoil condition is believed to be adequately representative of rotor blades in actual service. If some degree of roughness is considered more realistic, an allowance for that condition can be added to the results presented herein.

In contrast with the assumption of fully turbulent boundary layers on the airfoil surfaces, there is evidence that significant extents of laminar flow may exist on production rotor blades during normal operation; e.g., reference 1. Drag estimation methods can be, and have been (reference 2) evolved that accord with such evidence. However, for the purpose of a minimally complicated calculation program, with good applicability to the performance capabilities of an aircraft throughout its lifetime, the subtleties of the transition problem have been bypassed. There is little hope of generalizing the assumption of a transition location on a given blade such that one's conclusion will be valid in day-to-day operations of the aircraft. The sum total of high Reynolds number, service wear, deposits from the environment, and atmospheric turbulence tend to make the

assumption of a fully turbulent boundary layer on the main rotor blades
an acceptably applicable, if slightly conservative, one.

The intended application of the airfoil profile drag estimation
method to performance predictions for rotary-wing aircraft does not, in
any way, detract from the greater universality of the method; i.e., to
fixed-wing aircraft as well.

DISCUSSION

Minimum Drag Coefficient:

The profile drag of an airfoil can be regarded as the sum of a friction drag, D_F , due to the tangential forces acting on the airfoil surfaces, and a pressure (or form) drag, D_S , due to the normal forces.

$$D = D_F + D_S = D_F \left(1 + \frac{D_S}{D_F}\right) \quad (1)$$

In coefficient form, $C_D = C_F \left(1 + \frac{C_S}{C_F}\right) \quad (2)$

Friction Drag:

The procedure used here to arrive at a convenient expression for the friction drag is to treat the airfoil as a flat plate, with surface length equal to the perimeter of the airfoil, in a stream of effective dynamic pressure equal to that of the average local dynamic pressure on the airfoil. Then,

$$D_F = C_f (q_L)_A (L) \text{ per unit span} \quad (3)$$

or, $C_F = C_f \left(\frac{q_L}{q_0}\right)_A \left(\frac{L}{c}\right) = C_f (S)_A \left(\frac{L}{c}\right) \quad (4)$

The mean skin friction coefficient, C_f , is taken to be that of a smooth flat plate in turbulent flow at a Reynolds number defined as

$$R_N = R_{N0} \left(1/2 \frac{L}{c}\right) \sqrt{(S)_A} \quad (5)$$

For this purpose, the Karman-Schoenherr equation for a fully turbulent flat plate is used,

$$\log (R_N C_f) = \frac{0.242}{\sqrt{C_f}} \quad (6)$$

Equation (6) is plotted as Figure 1. A table of values of C_f versus R_N , computed at small intervals of R_N , can be found in reference 3.

Pressure Drag:

The airfoil pressure drag is taken to be the difference between the friction drag as computed above and measured test values of profile drag. The airfoil test data of references 4, 5, and 6 are used for this purpose.

A difficulty arises from the fact that test data for smooth airfoils with fully turbulent boundary layers are not available. The data are either for smooth airfoils with extensive, and undetermined, amounts of laminar flow, or for airfoils with roughness on their leading edges to insure fully turbulent flow. For the present purpose, the latter data are used, with an estimate of the incremental drag attributable to the roughness deducted from the test values. The remainder is considered as the equivalent of a smooth profile in fully turbulent flow. It is the difference between the profile drag, so determined, and the computed friction drag, that is considered to represent the airfoil pressure drag.

In a perfect flow there is no boundary layer and, therefore, no pressure drag. In an actual flow the boundary layer effectively distorts the profile, inhibits full pressure recovery at the airfoil trailing edge, and accounts for a net drag due to normal pressures, whether flow separation is present or not. The pressure drag, at $\alpha = 0^\circ$, is, therefore, closely related to the size and shape of the boundary layer on the profile. The skin friction coefficient is also related to the boundary layer thickness; e.g., using the 1/7-power law for a turbulent boundary layer,

$$\frac{d}{x}^* = \frac{0.046}{\sqrt{RN_x}} \quad \text{and, } C_f = \frac{0.072}{\sqrt{RN_x}}$$

so that, $\frac{C_f}{\delta^{*2}/x} = \text{constant}$.

On the basis of the preceding, it is reasoned that the magnitude of the airfoil pressure drag is related to that of the friction drag at zero degrees of airfoil attitude, where flow separation is either nonexistent or very limited. Consequently, these drags are expressed in the form of a ratio, as in Equations (1) and (2.)

Analysis:

The test data used in the present analysis (Table I) were all obtained at a $R_{N0} = 6 \times 10^6$ with NACA standard roughness (0.011-inch sand grains) distributed over each surface from the airfoil leading edge to a distance aft equivalent to $0.08c$. In order to implement the procedure described above and solve Equation (4) for each of the test airfoils it was necessary to determine L/c and $(S)_A$ in each case, as shown in Figures 2 and 3. These and other pertinent data are also listed in Table I. The values in Figure 3 were obtained from the theoretical pressure distributions presented in references 4 and 5. The distributions for the 4-digit family of airfoils, reference 4, were modified at the trailing edge, rather than assumed to return to a stagnation condition. This modification provides an allowance for the existence of boundary layers.

Figures 1, 2, and 3, with the R_N defined as in Equation (5,) provide the information needed to solve Equation (4) for values of friction drag coefficient for smooth airfoils with fully turbulent boundary layers. For precise values of C_f , reference 3 or a solution of Equation (6) is recommended in place of Figure 1. The results of such computations are listed in Table I and shown for a typical airfoil family, the 64-series,

in Figure 4, with the label C_{FS} . The considerable difference between these results and the test data points plotted in Figure 4, indicates a sizeable effect due to the roughness grains on the test airfoils.

The method used to estimate the drag increment, $(\Delta C_F)_R$, due to the roughness on the test airfoils is described in Appendix A. The results are listed in Table I. An example of the total friction drag coefficient, C_F , computed for 64-series airfoils with NACA standard roughness at $R_{N0} = 6 \times 10^6$ is shown in Figure 4, where,

$$C_F = C_{FS} + (\Delta C_F)_R \quad (7)$$

The pressure drag coefficient, C_S , was taken to be the difference between the test data and the computed values of C_F . Those differences were divided by the computed C_F 's, and the ratio, C_S/C_F , obtained in each case, was plotted in Figure 5. Unfortunately, the cumulative effects of scatter among the test data, and any other errors, are concentrated in Figure 5. Since possible errors of a few percent are of the same order of magnitude as C_S/C_F , the individual points in Figure 5 cannot be regarded as precise. To retain generality, with probable errors no greater than about 2-percent of the airfoil profile drag, a single curve has been drawn on Figure 5 to be used for estimation purposes (e.g., C_{DS} calculated in Table I.)

The preceding paragraphs have covered a method for the estimation of smooth, symmetrical airfoil minimum profile drag coefficient at any Reynolds number and low subsonic Mach number. Test data with which to

either substantiate or disprove the method are not available. An alternative attempt to verify the procedure, in itself a possible means of arriving at the same desired end, is presented in Appendix B.

Compressibility Effects:

The airfoil data used in the analyses were obtained at Mach numbers of less than 0.2. Test data, in general, indicate very little effect of Mach number, below the drag rise value, on airfoil minimum drag coefficient. The small effects of this Mach number range on the drag are frequently masked by the effects of variations in the Reynolds number as well, or, for smooth airfoils, by changes in the boundary layer transition positions on the airfoil surfaces with Mach number, or simply by the limitations of measurement accuracy.

Examination of Equation (4) suggests that the Mach number effect on airfoil friction coefficient can be expressed as,

$$\frac{C_{F_c}}{C_{F_1}} = \frac{C_{f_c}}{C_{f_1}} \frac{(S_c)_A}{(S_1)_A} \quad (8)$$

The effect of Mach number on the turbulent skin friction coefficient of a flat plate has been the subject of numerous investigations. For Mach numbers up to 0.8 or 0.9 the effects are small and can be represented adequately for the present purpose, from the test results of reference 7, by

$$\frac{C_{f_c}}{C_{f_1}} = 1 - .08 (M)^{1.75} \quad (9)$$

The Prandtl-Glauert similarity rule can be applied to the low Mach number values of S_A to yield,

$$\frac{(S_c)_A}{(S_1)_A} = \sqrt{\frac{1-M_1^2}{1-M_c^2}} + \frac{1}{(S_1)_A} \left(1 - \sqrt{\frac{1-M_1^2}{1-M_c^2}} \right) \quad (10)$$

Typical results obtained by combining the above two effects are (assuming $M_1 = 0.20$):

(1) NACA 64₂-015 airfoil at $M = 0.70$:

$$\frac{C_{f_c}}{C_{f_1}} = 0.957 \quad \frac{(S_c)_A}{(S_1)_A} = 1.028$$

$$\therefore \frac{C_{F_c}}{C_{F_1}} = 0.984$$

(2) NACA 64-006 airfoil at $M = 0.85$:

$$\frac{C_{f_c}}{C_{f_1}} = 0.940 \quad \frac{(S_c)_A}{(S_1)_A} = 1.067$$

$$\therefore \frac{C_{F_c}}{C_{F_1}} = 1.003$$

Assuming that C_S/C_F is independent of Mach number below the drag rise value, it is apparent that an increase in Mach number, prior to the onset of local shocks on the airfoil, has very little effect on the airfoil profile drag coefficient. The effects of Mach number on the onset and the magnitude of the drag rise have been the subject of numerous studies and data correlations and are not discussed here.

Profile Drag Due to Lift:

The test data of references 4, 5, and 6 were examined to determine the variation of section profile drag coefficient with angle of attack. Significant effects of airfoil family, thickness, Reynolds number, and surface condition were noted. This multiplicity of factors precludes a precise, yet simple, generalization. However, with some sacrifice in accuracy, a relatively simple method has been evolved which can be used to estimate the increment in profile drag coefficient due to angle of attack for smooth airfoils with fully turbulent boundary layers.

The test data at $R_{NO} = 6 \times 10^6$, with NACA standard roughness on the airfoil surfaces, were used for the present analysis. First, the roughness effect was estimated and subtracted from the test data, in the manner previously described under "Minimum Drag Coefficient." Since the pressure distribution changes with angle of attack, particularly near the airfoil leading edge, the incremental drag due to the roughness must itself be a function of α . A study was made of the effects of α on the theoretical pressure distributions. From these results, the increase in the average value of S over the roughened region of the test airfoils was determined. Application of these results defines the incremental drag due to roughness, in the test data; e.g., Figure 6. This effect of roughness was subtracted from the test data (standard roughness) for each airfoil, and the resulting drag curve assumed equivalent to that of a smooth airfoil with fully turbulent boundary layers.

The airfoil data, adjusted from the rough to smooth condition as above, were examined for potential generalization of their variations of C_D with α in a reasonably simple manner. The result, for $R_{N0} = 6 \times 10^6$, is an equation of the form,

$$(\Delta C_D)_\alpha = K(\alpha)^{2.7} \quad (11)$$

where α is in radians, and K is a function of thickness as shown in Figure 7.

The effect of Reynolds number on airfoil drag coefficient at any angle of attack can be estimated by assuming C_S/C_F independent of R_N at a given angle of attack, as was done for $\alpha = 0^\circ$. Then $C_D \sim C_F \sim C_f$. It follows that $(\Delta C_D)_\alpha \sim C_f$, so that,

$$(\Delta C_D)_\alpha = \frac{(C_f)_{R_{Neff}}}{[(C_f)_{R_{Neff}}]_{R_{N0} = 6 \times 10^6}} K(\alpha)^{2.7} \quad (12)$$

The variation of C_f with α , due to an increase in S_A with α , and, therefore, an increase in effective R_N , will be small, and is accounted for, to some extent, in Equation (11). Therefore, it is recommended that values of C_f determined for effective values of R_N at $\alpha = 0^\circ$ be used in the solution of Equation (12).

Equations (2), (4), and (12) combined yield the expression for airfoil profile drag coefficient,

$$C_D = [(C_f)_{R_{Neff}}]_{\alpha = 0^\circ} \left\{ (S_A)_{\alpha = 0^\circ} \left(\frac{L}{c} \right) \left[1 + \left(\frac{C_S}{C_F} \right)_{\alpha = 0^\circ} \right] + \frac{K(\alpha)^{2.7}}{[(C_f)_{R_{Neff}}]_{(R_{N0} = 6 \times 10^6, \alpha = 0^\circ)}} \right\} \quad (13)$$

Examples of the results of applying Equation (13) to the NACA 64₁-012 airfoil are shown in Figure 8.

Effect of Camber:

A study of airfoil data reveals little or no effect of camber on the value of the minimum drag coefficient or its occurrence at $\alpha = 0^\circ$. The effect of α in the range below the stall value is similar to its effect on the uncambered section. Consequently, with good accuracy, the relation of C_D versus α obtained from Equation (13) for an uncambered airfoil can be applied to an airfoil with the same thickness distribution but a cambered mean line. The section lift curve will be shifted, and the magnitude of the shift can be very closely approximated by the result from thin airfoil theory,

$$\alpha_{OL} = -2(57.3) \left(\frac{\text{maximum camber}}{c} \right) \text{ in degrees.}$$

Profile Drag Beyond Stall Angle:

At airfoil angles of attack greater than the stall attitude, the profile drag is relatively independent of Reynolds number and the airfoil's thickness and shape. Test data for an NACA 0012 airfoil, reference 8, and a flat plate, reference 9, obtained in the stalled flow regime ($\alpha > 20^\circ$), can be correlated by

$$C_D = 2.1(\sin \alpha)^{1.7} \tag{14}$$

as shown in Figure 9.

The complete profile drag curve for a symmetrical airfoil, ($-90^\circ \leq \alpha \leq 90^\circ$), can be constructed if the stall angle for the airfoil, at the given flow conditions, is known. Equation (13) can be used for angles of attack below

the stall and Equation (14) for angles above the stall. An example is shown in Figure 10 for the NACA 0012 airfoil. A rapid transition between the two curves is expected in the stall onset region.

RECOMMENDED ESTIMATION PROCEDURE

Example: Calculate the drag coefficient versus angle of attack below stall, for the NACA 641-012 airfoil without roughness, with turbulent boundary layers, at a Reynolds number of 20×10^6 , based on free-stream velocity and the airfoil chord.

Solution:

$$(S_A)_{\alpha = 0^\circ} = 1.163 \text{ from Figure 3}$$

$$\frac{L}{c} = 2.0305 \text{ from Figure 2}$$

$$\left(\frac{C_S}{C_F}\right)_{\alpha = 0^\circ} = 0.037 \text{ from Figure 5}$$

$$K = 1.55 \text{ from Figure 7}$$

$$R_{N_{\text{eff}}} = R_{N_0} \times 1/2 \left(\frac{L}{c}\right) \sqrt{(S_A)_{\alpha = 0^\circ}} \text{ from Equation (5)}$$

$$\therefore R_{N_{\text{eff}}} = 21.9 \times 10^6 \text{ at } R_{N_0} = 20 \times 10^6$$

$$R_{N_{\text{eff}}} = 6.565 \times 10^6 \text{ at } R_{N_0} = 6 \times 10^6$$

$$\text{Then, } (C_f)_{R_{N_{\text{eff}}}} = 0.00259 \text{ from Figure 1}$$

$$\left[(C_f)_{R_{N_{\text{eff}}}}\right]_{(R_{N_0} = 6 \times 10^6, \alpha = 0^\circ)} = 0.00315 \text{ from Figure 1}$$

Substituting these values in Equation (13) yields,

$$C_D = 0.00634 + 0.000023 (\alpha)^{2.7}$$

with α in degrees.

The solution of this equation is plotted on Figure 8.

New and/or Untested Airfoils:

Application of the method presented in this paper is straightforward for airfoils included in the families used as examples herein (4-Digit and 6-Series). Extension of the same estimation procedure to an airfoil shape not included in Figures 2 and 3 requires the determination of the airfoil's perimeter and average pressure coefficient. The perimeter is an obviously measurable quantity. The determination of the average pressure coefficient requires an estimate of the airfoil pressure distribution. That can be limited to the pressure distribution on one surface, at $\alpha = 0^\circ$, for an airfoil with the given thickness distribution only. The airfoil's camber can be neglected for this purpose, since its opposing effects on the upper and lower airfoil surfaces are essentially self-cancelling.

TABLE I

AIRFOIL MINIMUM DRAG CALCULATIONS

Airfoil NACA-	L/c Fig 2	SA Fig 3	(Cd) Test R _{No} -6x106 Std Rough	R _N x10 ⁻⁶ effect Eq (5)	C _f s Eq (6)	C _f s Eq (4)	(ΔC _p) _R App A	C _f Eq (7)	C _s /C _f	C _d s Calc (Use curve in Fig 5)
0006	2.0107	1.096	.00885	6.32	.00317	.00698	.00158	.00856	.0339	.00704
0009	2.023	1.146	.0091	6.50	.00315	.00731	.00162	.00893	.0190	.00745
0012	2.0374	1.192	.0098	6.675	.00314	.00763	.00162	.00925	.0594	.00791
63-006	2.0095	1.082	.00865	6.27	.00317	.00689	.00148	.00837	.0335	.00695
63-009	2.0192	1.122	.00875	6.415	.00316	.00716	.00151	.00876	.0092	.00730
631-012	2.0318	1.164	.0092	6.577	.00315	.00745	.00150	.00895	.0279	.00773
632-015	2.0465	1.202	.0096	6.735	.00314	.00771	.00147	.00918	.0458	.00823
633-018	2.0637	1.242	.01035	6.903	.00312	.0080	.00141	.00941	.1000	.00883
634-021	2.0817	1.280	.0109	7.063	.00311	.00829	.00131	.0096	.1354	.00949
64-006	2.0089	1.082	.0085	6.268	.00317	.00689	.00149	.00838	.0143	.00695
64-009	2.0185	1.122	.0087	6.411	.00316	.00715	.00152	.00867	.0035	.00729
641-012	2.0305	1.163	.00905	6.565	.00315	.00743	.00151	.00894	.0123	.00770
642-015	2.0452	1.202	.00965	6.727	.00314	.00771	.00147	.00918	.0512	.00823
643-018	2.062	1.242	.0103	6.897	.00312	.0080	.00142	.00942	.0934	.00883
644-021	2.0796	1.281	.01065	7.064	.00311	.00829	.00132	.00961	.1082	.00949
65-006	2.0084	1.084	.0082	6.272	.00317	.0069	.00146	.00836	.0192	.00696
65-009	2.0176	1.127	.0088	6.428	.00316	.00718	.00147	.00865	.0173	.00732
651-012	2.0287	1.170	.00915	6.585	.00315	.00747	.00147	.00894	.0235	.00775
652-015	2.0429	1.209	.0099	6.742	.00314	.00774	.00143	.00917	.0796	.00826
653-018	2.0586	1.248	.0105	6.899	.00312	.00802	.00138	.0094	.1170	.00885
654-021	2.076	1.289	.01095	7.069	.00311	.00832	.00129	.00961	.1394	.00953
66-006	2.0084	1.086	.00835	6.278	.00317	.00691	.00144	.00835	0	.00697
66-009	2.0177	1.127	.0090	6.428	.00316	.00718	.00146	.00864	.0417	.00732
661-012	2.029	1.170	.0094	6.586	.00315	.00747	.00146	.00893	.0526	.00775
662-015	2.0434	1.213	.00995	6.749	.00314	.00777	.00142	.00919	.0827	.00829
663-018	2.0595	1.254	.01065	6.92	.00312	.00806	.00137	.00943	.1294	.00890
664-021	2.077	1.294	.0119	7.091	.00311	.00836	.00127	.00953	.2357	.00957
64A010	2.022	1.145	.0092	6.491	.00316	.0073	.0015	.0088	.0454	.00748

FIGURE 1

SKIN FRICTION DRAG OF FLAT PLATE

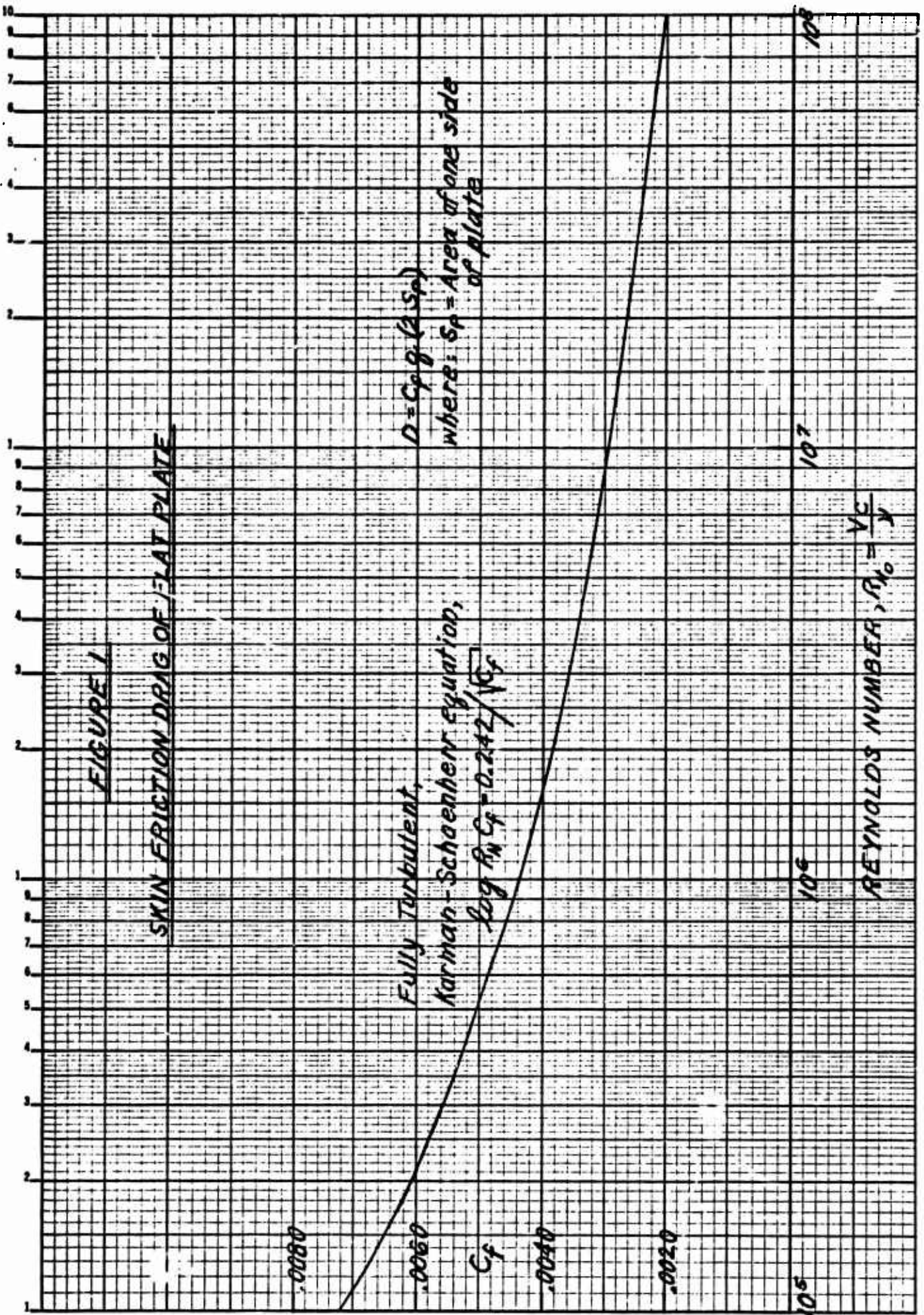
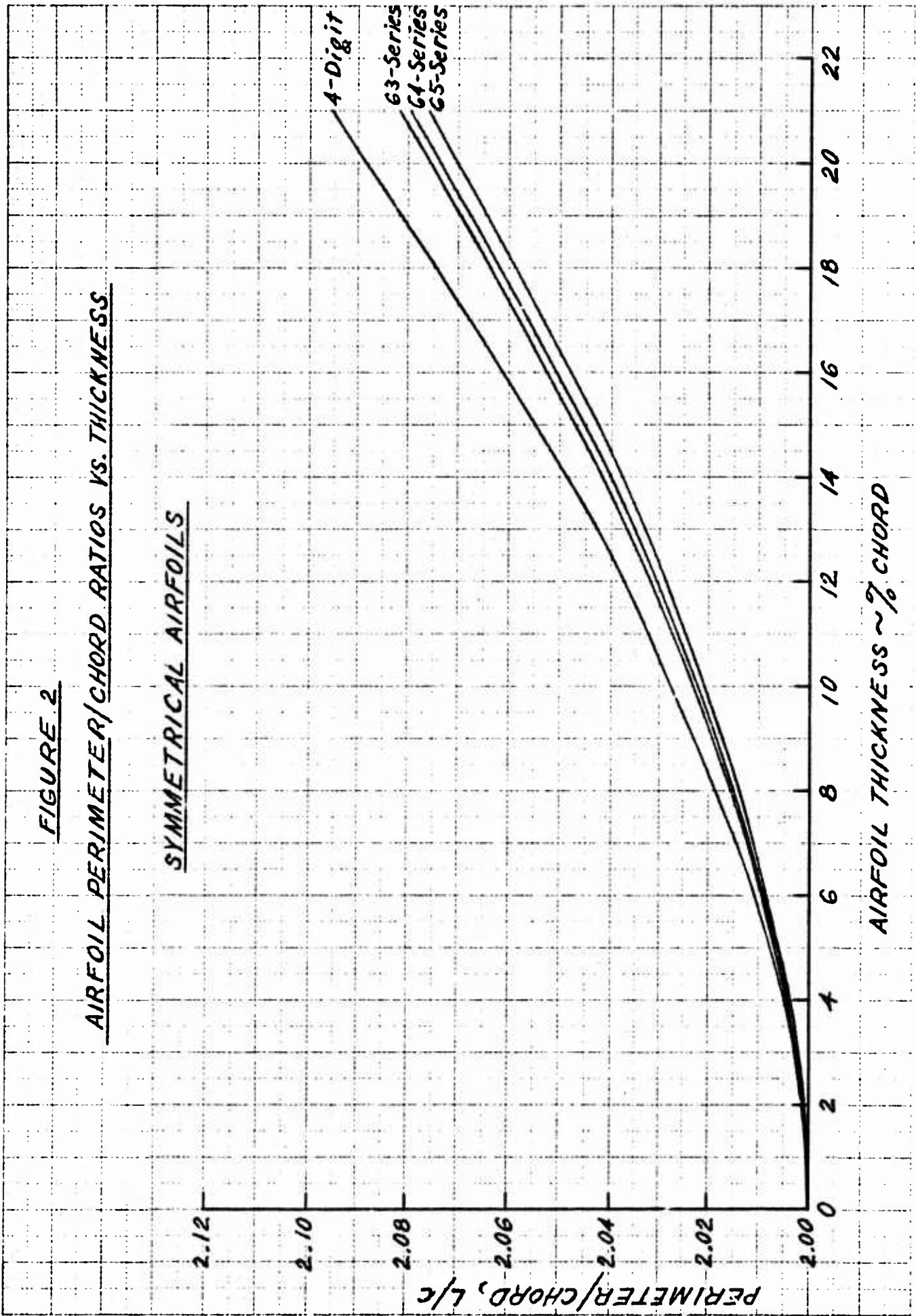


FIGURE 2

AIRFOIL PERIMETER/CHORD RATIOS VS. THICKNESS

SYMMETRICAL AIRFOILS



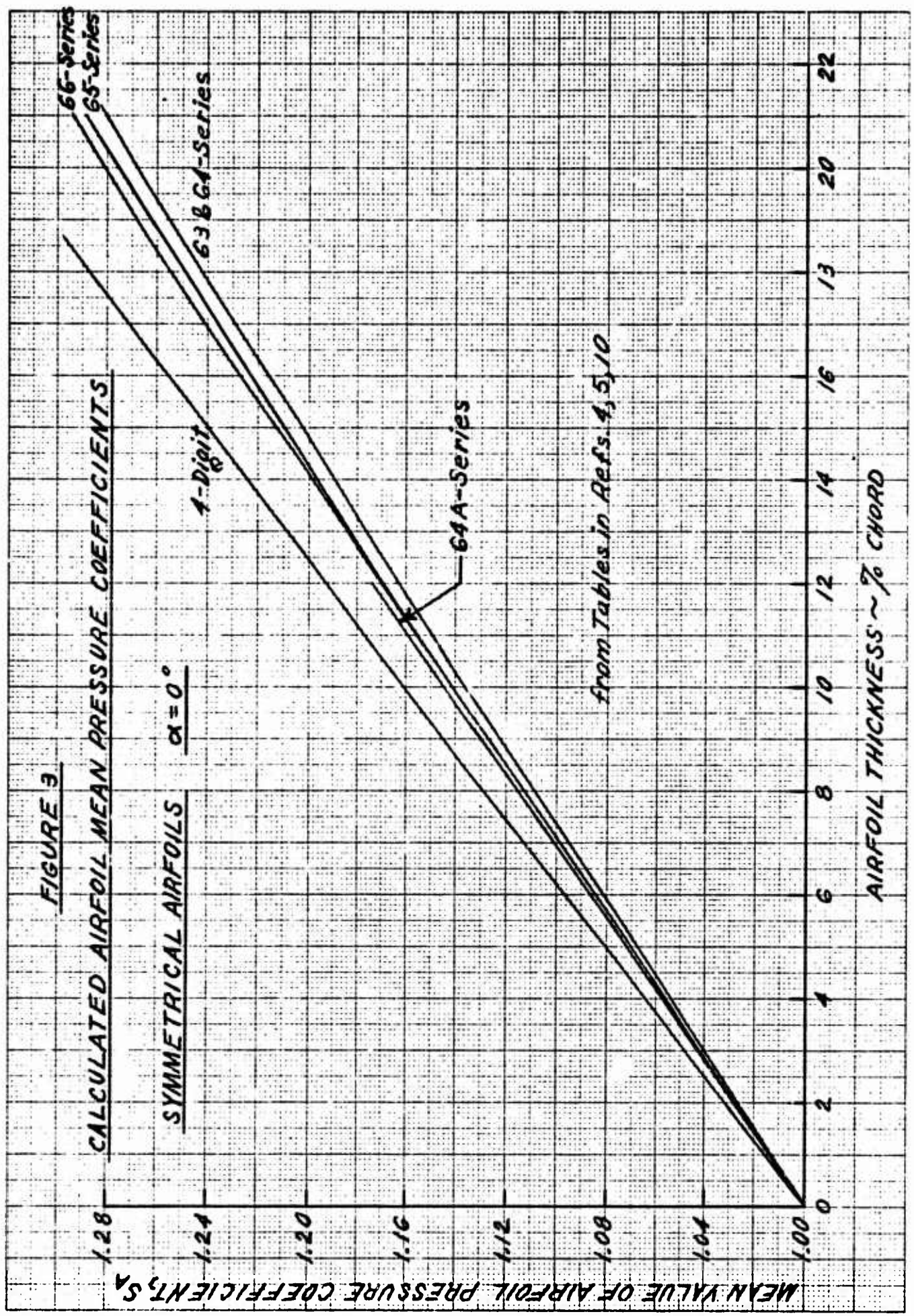


FIGURE 4

DRAG COEFFICIENTS OF 64-SERIES AIRFOILS

SYMMETRICAL AIRFOILS $\alpha = 0^\circ$ $R_{N_0} = 6 \times 10^6$

○ Measured C_D with NACA
standard roughness, Ref. 4

— Calculated

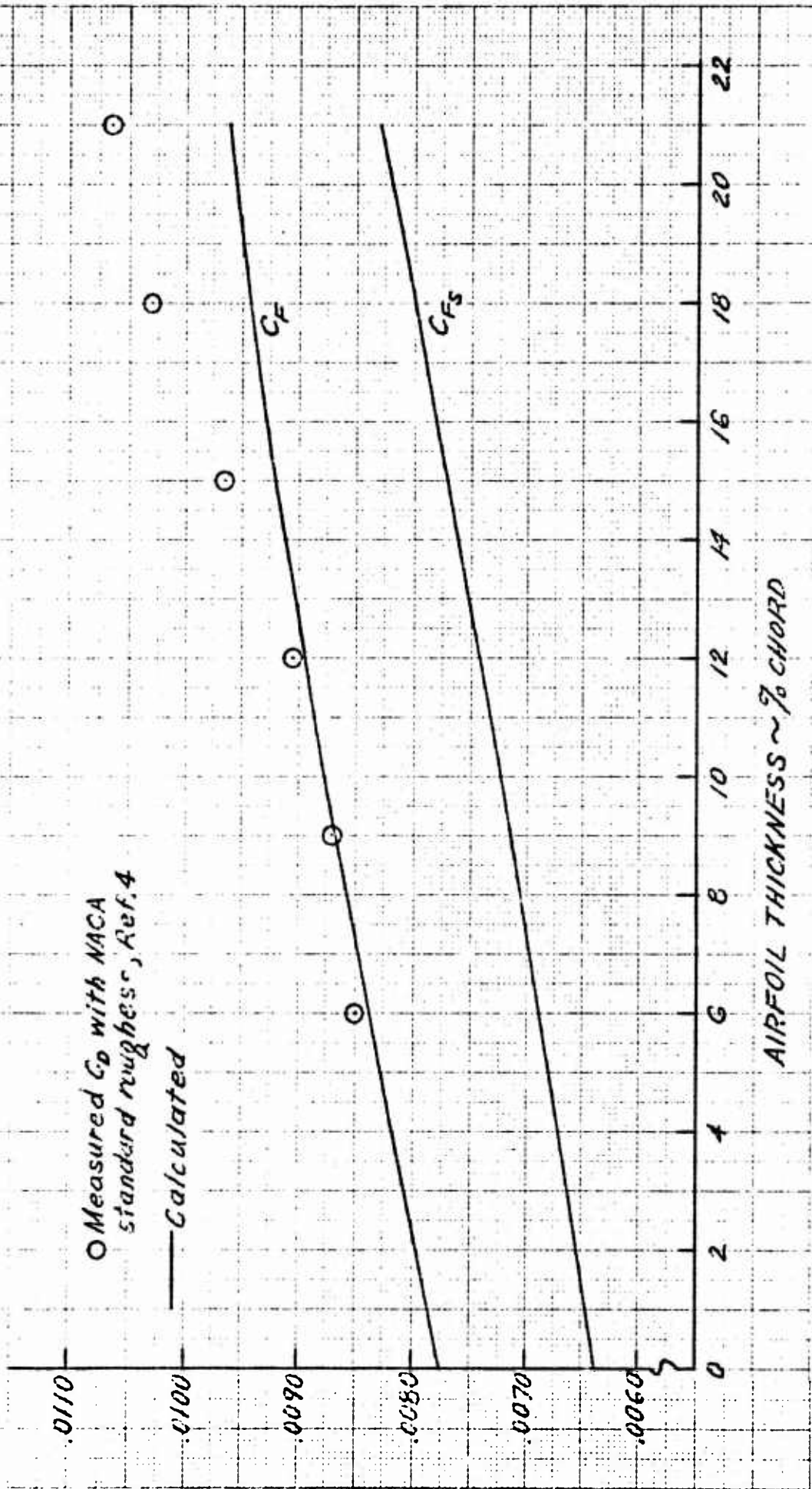


FIGURE 5

FORM DRAG/FRICTION DRAG VS. AIRFOIL THICKNESS

SYMMETRICAL AIRFOILS $\alpha = 0^\circ$

AIRFOIL SERIES

- 4-Digit
- △ 63-
- 64-
- ▽ 65-
- ◇ 66-
- 64A-



FIGURE 6

ESTIMATED INCREMENTAL AIRFOIL DRAG
COEFFICIENT DUE TO LEADING-EDGE ROUGHNESS

SYMMETRICAL AIRFOILS $P_{N0} = 6 \times 10^6$

NACA Standard Roughness (0.011" sand grains)
over 0.08c from leading edge on each surface

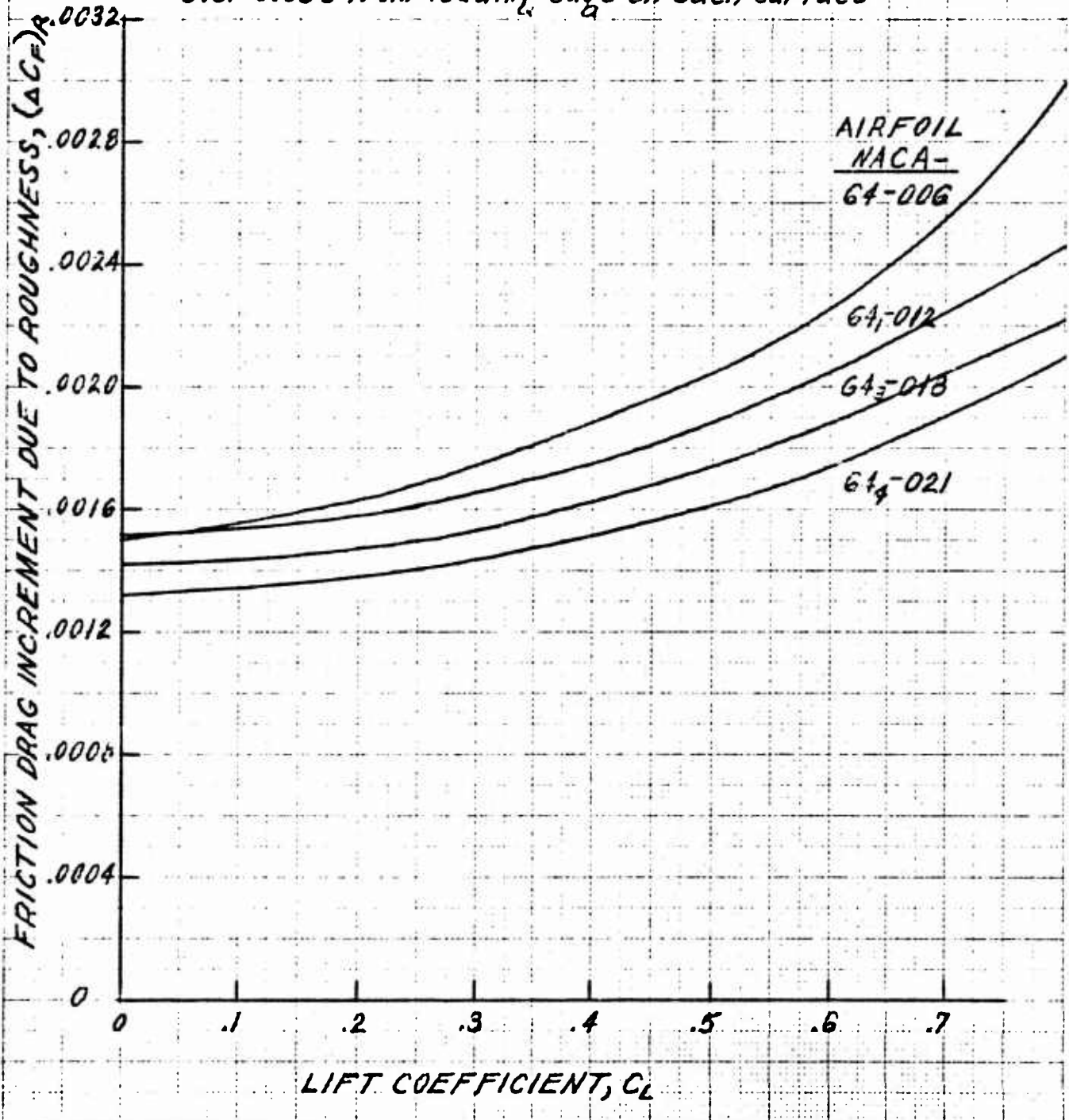


FIGURE 7

AIRFOIL DRAG DUE TO LIFT

CORRELATION PARAMETER

$R_{N_0} = 6 \times 10^6$

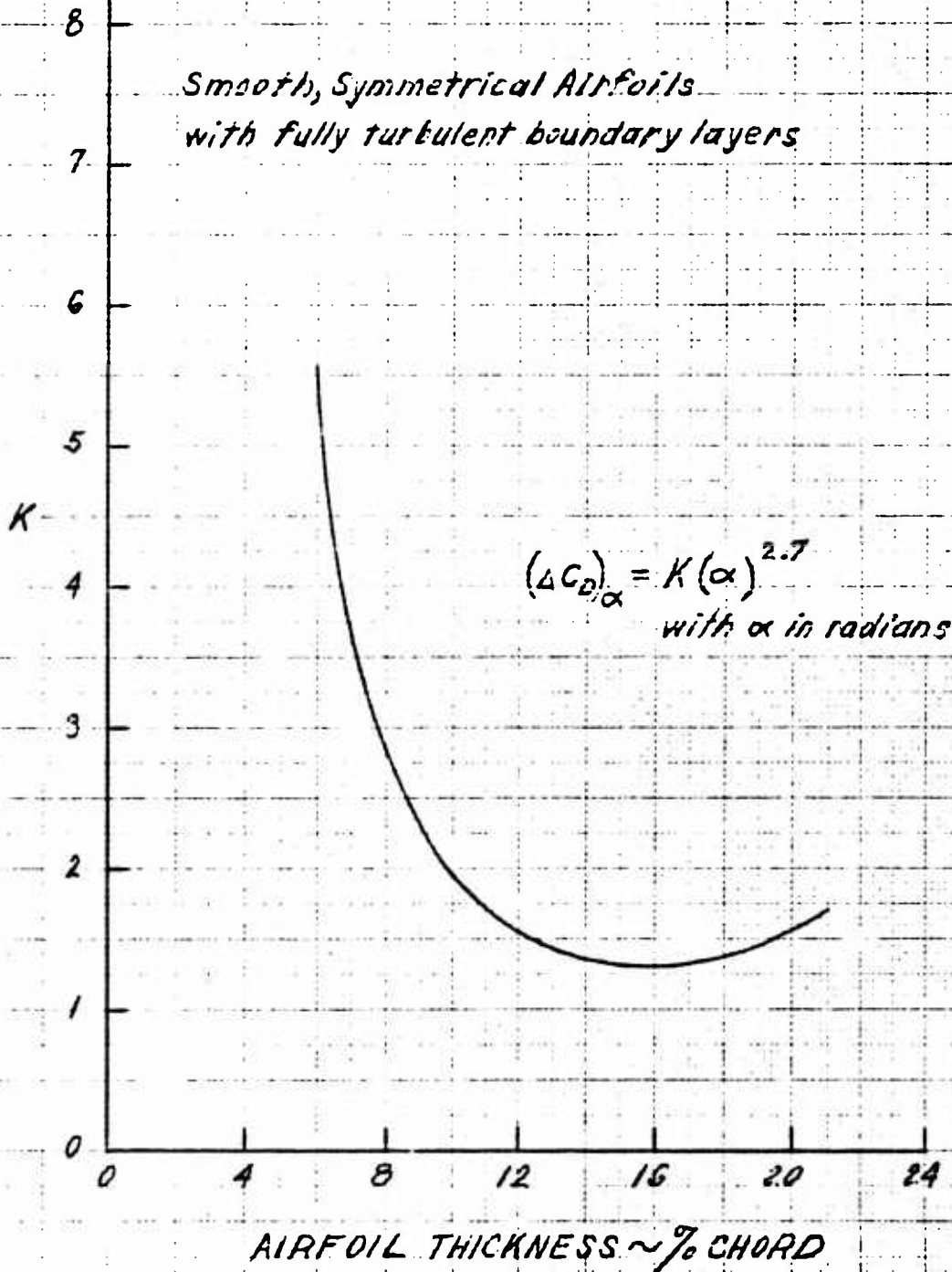
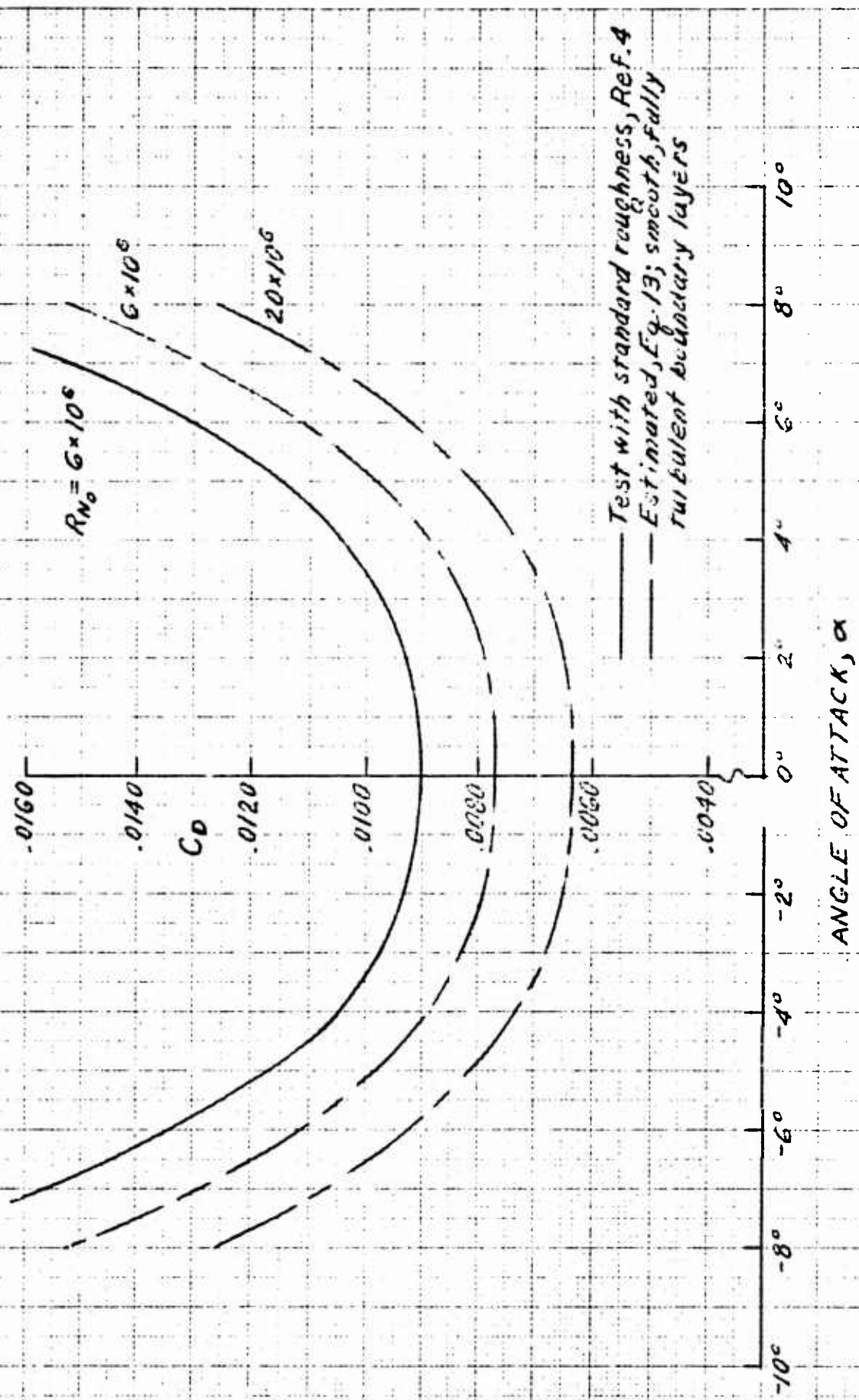
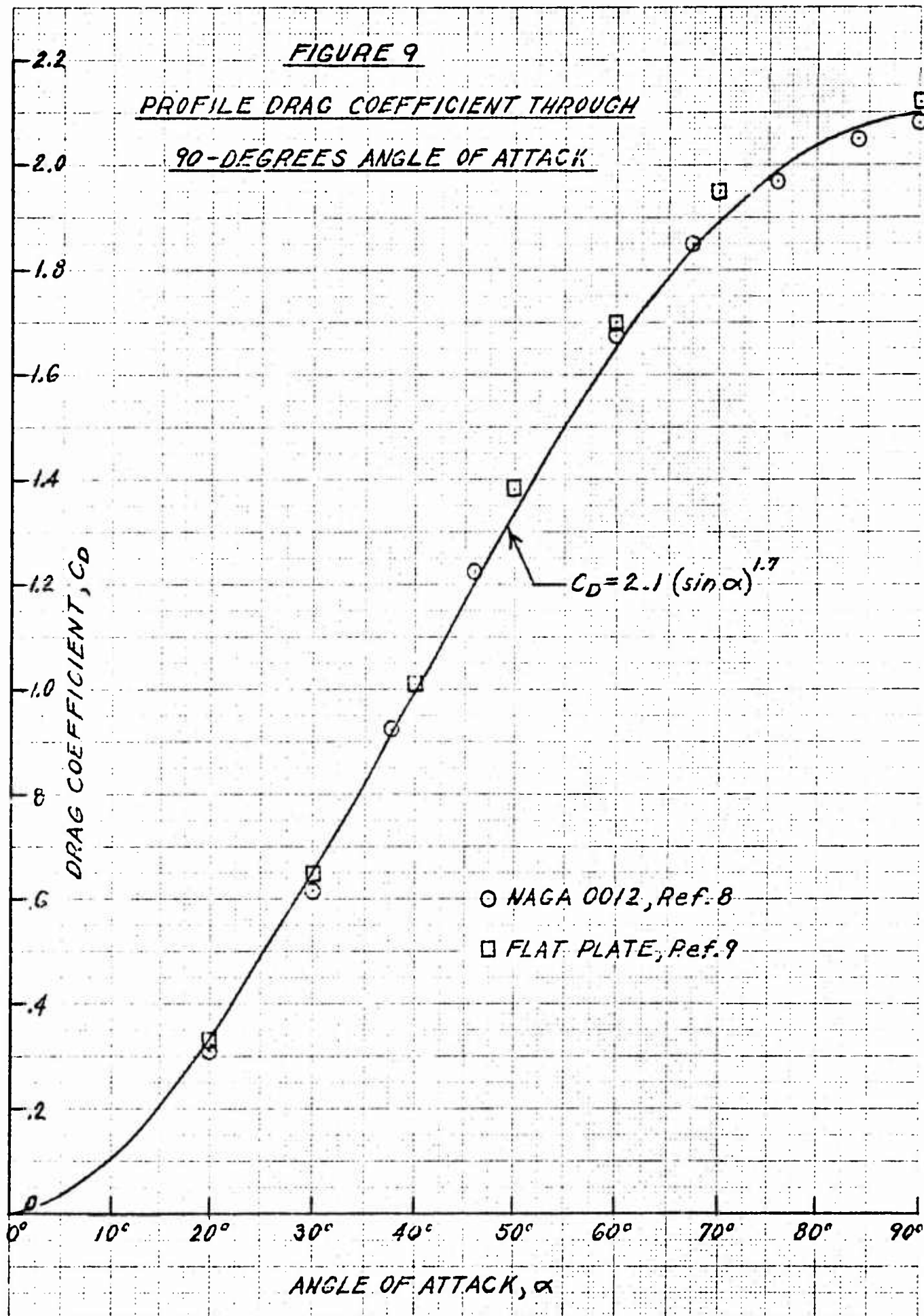
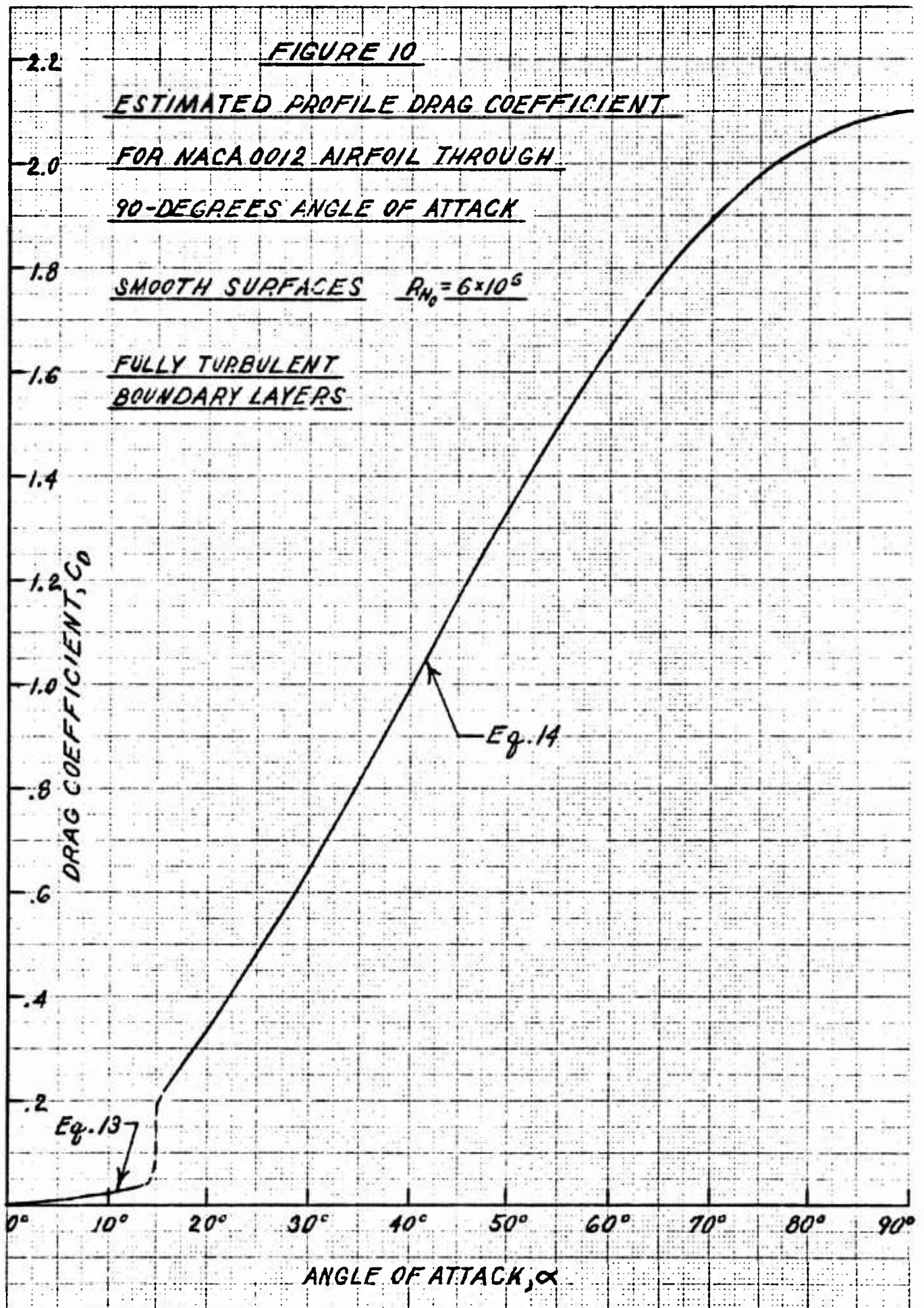


FIGURE 8

DRAG COEFFICIENTS OF NACA 64-012 AIRFOIL







REFERENCES

1. Tanner, W. H. and Yaggy, P. F., EXPERIMENTAL BOUNDARY LAYER STUDY ON HOVERING ROTORS, AHS 22nd Annual National Forum Proceedings, May 1966, pp. 13-28.
2. Cebeci, T. and Smith, A. M. O., CALCULATION OF PROFILE DRAG OF AIRFOILS AT LOW MACH NUMBERS, Journal of Aircraft, Volume 5, No 6, November - December 1968, pp. 535-542.
3. Locke, F. W. S., Jr., RECOMMENDED DEFINITION OF TURBULENT FRICTION IN INCOMPRESSIBLE FLUIDS, NAVAER DR Report 1415, Bur Aero, June 1952.
4. Abbott, I. H., von Doenhoff, A. E., and Stivers, L. S., Jr., SUMMARY OF AIRFOIL DATA, NACA Report 824, 1945.
5. Loftin, L. K., Jr., THEORETICAL AND EXPERIMENTAL DATA FOR A NUMBER OF NACA 6A-SERIES AIRFOIL SECTIONS, NACA Report 903, 1948.
6. Loftin, L. K., Jr. and Smith, H. A., AERODYNAMIC CHARACTERISTICS OF 15 NACA AIRFOIL SECTIONS AT SEVEN REYNOLDS NUMBERS FROM 0.7×10^6 TO 9.0×10^6 , NACA TN 1945, 1949.
7. Chapman, D. R. and Kester, R. H., TURBULENT BOUNDARY-LAYER AND SKIN-FRICTION MEASUREMENTS IN AXIAL FLOW ALONG CYLINDERS AT MACH NUMBERS BETWEEN 0.5 AND 3.6, NACA TN 3097, 1954.
8. Critzos, C. C., Heyson, H. H., and Boswinkle, R. W., Jr., AERODYNAMIC CHARACTERISTICS OF NACA 0012 AIRFOIL SECTION AT ANGLES OF ATTACK FROM 0° TO 180° , NACA TN 3361, 1955.
9. Wick, B. H., STUDY OF THE SUBSONIC FORCES AND MOMENTS ON AN INCLINED PLATE OF INFINITE SPAN, NACA TN 3221, 1954.

10. Patterson, E. W. and Braslow, A. L., ORDINATES AND THEORETICAL PRESSURE-DISTRIBUTION DATA FOR NACA 6- AND 6A-SERIES AIRFOIL SECTIONS WITH THICKNESSES FROM 2 TO 21 and FROM 2 TO 15 PERCENT CHORD, RESPECTIVELY, NACA TN 4322, 1958.
11. SCHLICHTING, H., BOUNDARY LAYER THEORY, McGraw-Hill Book Co, Inc, NY, First English Edition, 1955.
12. Abbott, F. T., Jr., and Turner, H. R., Jr., THE EFFECTS OF ROUGHNESS AT HIGH REYNOLDS NUMBERS ON THE LIFT AND DRAG CHARACTERISTICS OF THREE THICK AIRFOILS, NACA ACR No L4H21, August 1944.

APPENDIX A

Estimation of Leading-Edge Roughness Effect on $C_{D\text{MIN}}$

The incremental friction drag coefficient due to the roughness grains on the test airfoils was estimated as follows:

(1) The figure of C_f versus Re_0 for a sand-roughened plate, on page 448 of reference 11, provides a comparison of rough and smooth values of skin friction drag coefficient.

(2) All of the test airfoils were of 24" chord and had 0.011" sand grains over 0.08 c on each surface, therefore, $\frac{s}{k} = \frac{.08(24)}{.011} = 174.5$.

(3) The plate Re_R equivalent to .08c airfoil surface length was taken to be:

$$Re_R = 6 \times 10^6 (.08) \sqrt{(S_A)_R} \approx 5 \times 10^5.$$

(4) A cross-plot of the curves in the figure of reference 10 yields:

$$C_{fR} = 0.01380 \text{ for } \frac{s}{k} = 174.5 \text{ at } Re_R = 5 \times 10^5$$

$$C_{fS} = 0.00517 \text{ for } \frac{s}{k} = \infty \text{ at } Re_R = 5 \times 10^5.$$

(5) The incremental friction drag coefficient due to the roughness was then taken to be (analogous to Equation (4)):

$$(\Delta C_F)_R = (C_{fR} - C_{fS}) (2 \times .08) (S_A)_R = 0.00138(S_A)_R \quad (A-1)$$

In order to follow the method outlined in the preceding steps, it is necessary to determine the average pressure coefficient on each airfoil over that section of the airfoil with roughness on it, i.e., $(S_A)_R$. Since the chordwise extent of the roughness varied with airfoil shape and

thickness, the chordwise station at which the roughness ended was determined for the various families. The theoretical pressure distributions were then used to determine the average values of S over those sections of each airfoil which were covered by the roughness grains. Equation (A-1) was then solved and some of the results are included in Table I.

To justify the above procedure for estimation of the incremental drag coefficient due to leading-edge roughness, an analysis was made of available test data for a 36 inch chord NACA 63(420)-422 airfoil tested at a stream $R_{N_0} = 26 \times 10^6$, reference 12. Three different sizes of sand grains were used in that test, each in turn spread over $0.08c$ equivalent length on each surface behind the leading edge. The test and estimated results are compared in Figure A-1. For the estimation purposes, Schlichting's curves were cross-plotted at a $R_N = 2 \times 10^6$, and $(S_A)_R$ was assumed to be 0.92 (extrapolation of 63-series curve computed as above). The latter number may not be precise for this cambered airfoil at a small positive lift coefficient, but the error is within the accuracy of the data. The available test points are very few but their magnitude and trend agree well with the estimated curve.

FIGURE A-1

CHECK OF METHOD FOR ESTIMATION OF
DRAG INCREMENT DUE TO ROUGHNESS

○ NACA 63(420)-422, $R_{N0} = 26 \times 10^6$, Leading-Edge roughness
over 0.08c surface length on each surface, Ref. 12

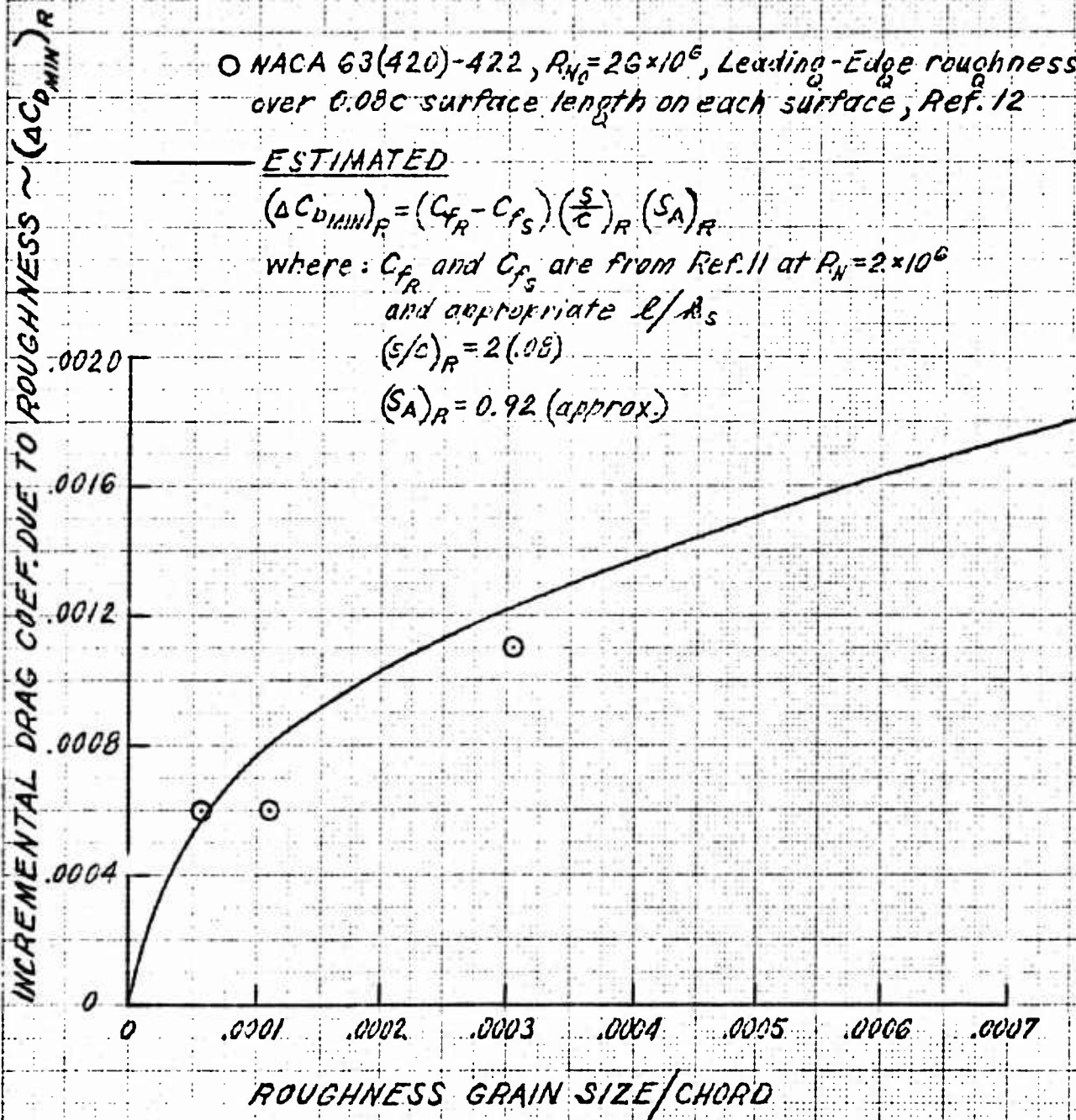
ESTIMATED

$$(\Delta C_{D_{MIN}})_R = (C_{fR} - C_{fS}) \left(\frac{s}{c}\right)_R (S_A)_R$$

where: C_{fR} and C_{fS} are from Ref. 11 at $R_N = 2 \times 10^6$
and appropriate l/A_s

$$\left(\frac{s}{c}\right)_R = 2(.08)$$

$$(S_A)_R = 0.92 \text{ (approx.)}$$



APPENDIX B

Alternative Method for Estimation of Minimum Profile

Drag of Smooth, Fully Turbulent, Symmetrical Airfoils

Test data are not available to verify the technique recommended in this report for the estimation of the profile drag coefficient of a smooth airfoil with fully turbulent flow. As an alternative means of achieving such verification, the method described below was used. It is, necessarily, another means of arriving at the same end; but, being dependent exclusively on test data, provides no general applicability in itself.

As an example, the 64-series airfoil test data presented in reference 4 will be used. These data were obtained with the airfoils in both the smooth and rough conditions at $R_{N0} = 6 \times 10^6$. A typical case of the NACA 641-012 airfoil is shown in Figure B-1.

For the smooth airfoil, the minimum drag coefficient is seen to be in the so-called "laminar flow bucket." Extensive amounts of laminar flow exist on both airfoil surfaces at $\alpha = 0^\circ$. A common practice in industry, in years past, was to fair out the "bucket" (as in Figure B-1) as unrealizable in practice, and use the faired value in its place. That portion of the drag curve outside of the "bucket" is at sufficiently high angles of attack for the adverse pressure gradient on the downwind side of the airfoil to have moved the boundary layer transition point on that surface forward to, or very close to, the leading edge. Simultaneously, the boundary layer on the upwind surface is little changed. Consequently,

the faired value should reasonably represent the minimum drag coefficient for the airfoil with essentially fully turbulent flow on one surface and the same, or nearly the same, extent of laminar flow on the other surface as for the unfaired data.

The drag increment between the value at the bottom of the "bucket" and the faired curve can be attributed, on the basis of the above, to movement of the boundary layer transition point on one surface up to the leading edge, while that on the other surface remains essentially unchanged. If this reasoning is followed one step further, we can conclude that a similar movement of the boundary layer transition point to the leading edge on the unaffected surface, so that both surfaces are in fully turbulent flow, would add another similar increment in drag.

The 64-series airfoils were examined in the context of the reasoning presented above. The results are shown in Figure B-2 and there compared to the profile drag coefficients calculated by means of the procedure outlined in this report for the same airfoil family with smooth surfaces and fully turbulent boundary layers. The good comparison obtained represents a qualitative approval of the presently recommended estimation method.

FIGURE B-1

DRAG COEFFICIENT VS. LIFT COEFFICIENT OF NACA 64,-012 AIRFOIL

$Re = 6 \times 10^6$ 24-inch chord

from Ref. 4

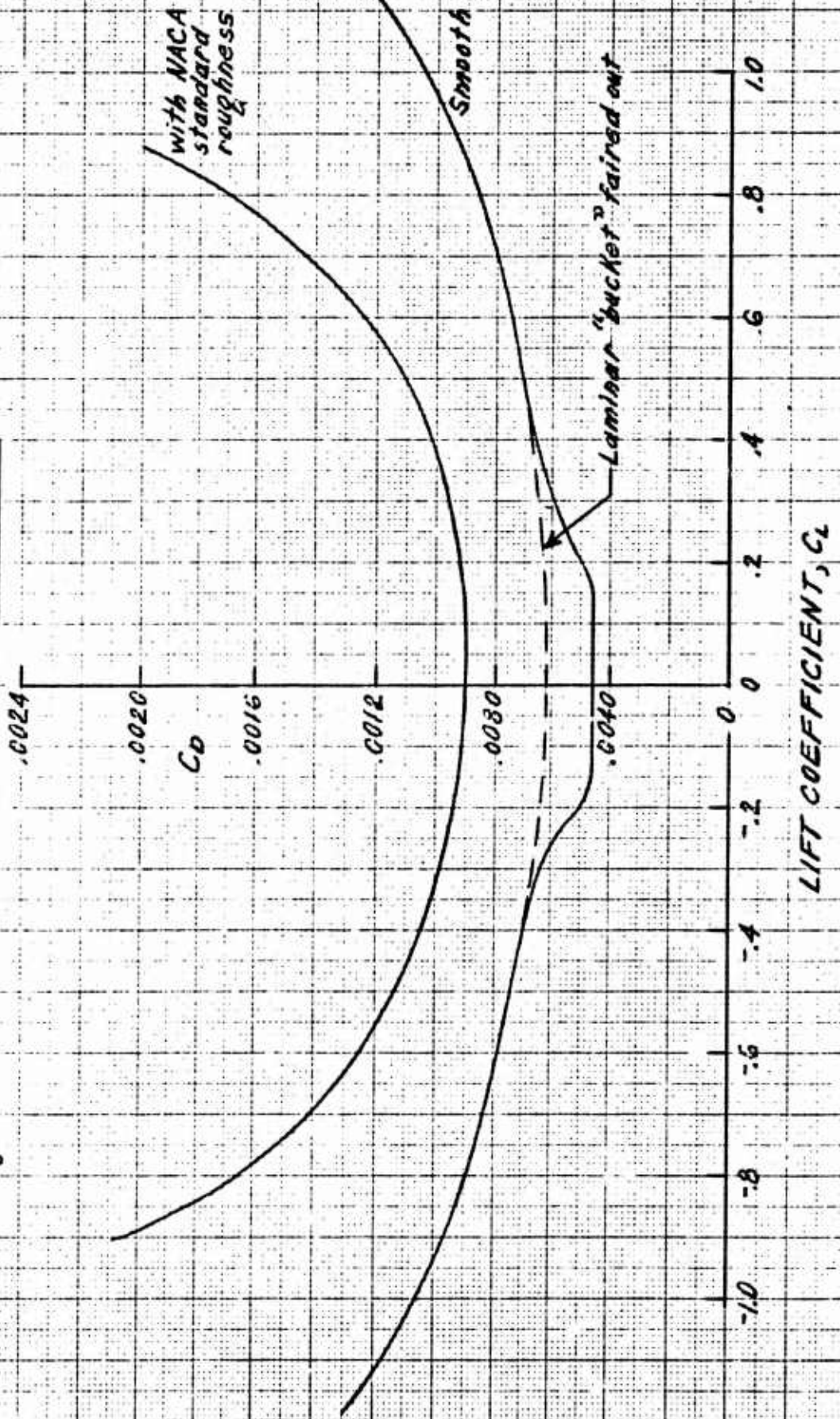
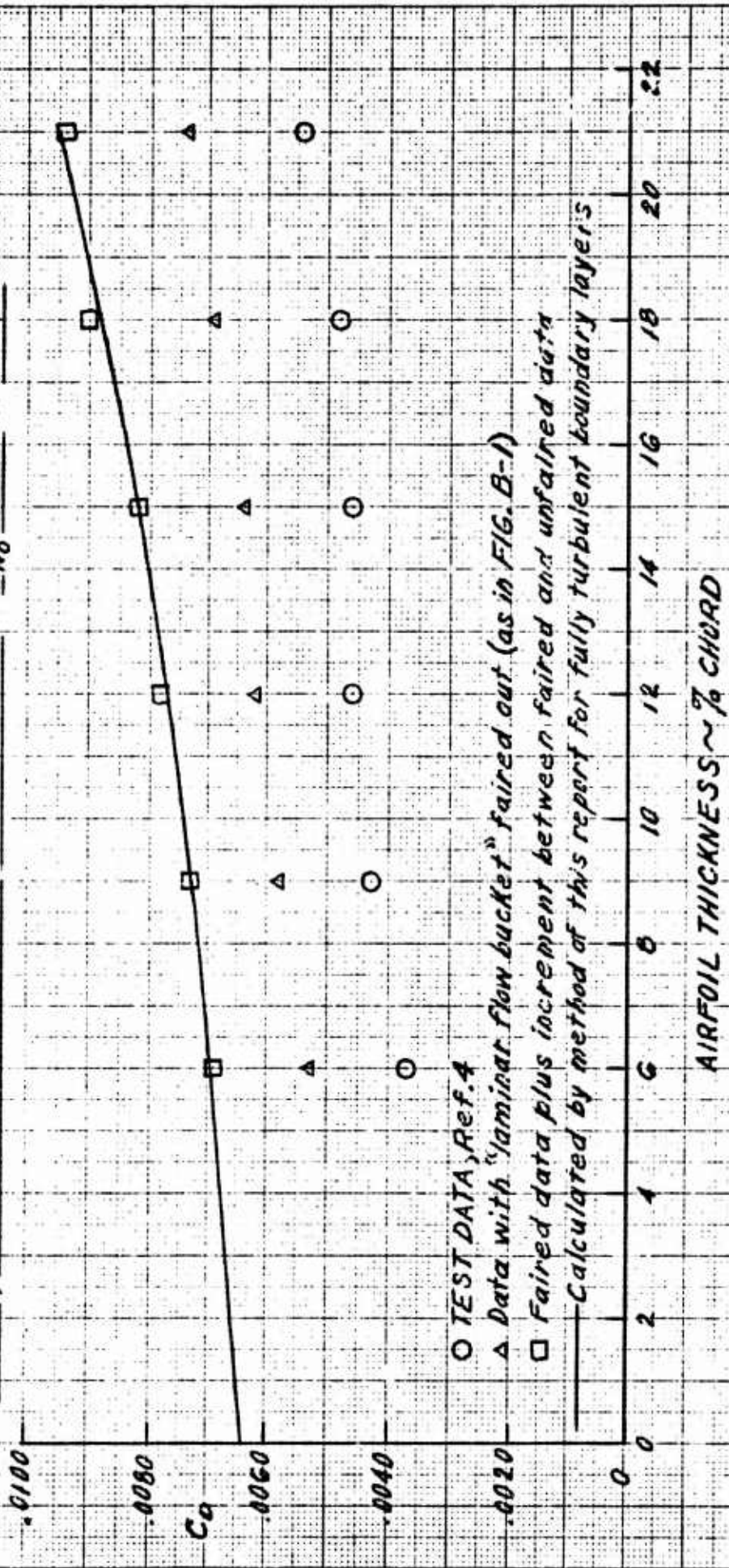


FIGURE B-2

CHECK OF PRESENT CALCULATION METHOD BY ALTERNATE

ESTIMATION PROCEDURE

SMOOTH, SYMMETRICAL NACA 64-SL 7IES AIRFOILS $R_{N0} = 6 \times 10^6$ $\alpha = 0^\circ$



○ TEST DATA, Ref. 4

△ Data with "laminar flow bucket" faired out (as in FIG. B-1)

□ Faired data plus increment between faired and unfaired data

— Calculated by method of this report for fully turbulent boundary layers

AIRFOIL THICKNESS ~ % CHORD

SYMBOLS

- c = Airfoil chord
- C_D = Profile drag coefficient
- C_F = Friction drag coefficient
- C_f = Average flat plate skin-friction coefficient
- C_L = Lift coefficient
- C_S = Pressure drag coefficient
- D = Drag
- D_F = Friction drag
- D_S = Pressure drag
- K = Coefficient in Equation (11) for profile drag due to lift
- k = Roughness grain size
- L = Perimeter of airfoil
- M = Mach number
- q = Dynamic pressure
- R_N = Reynolds number
- S = Pressure coefficient, $(V_L/V_0)^2$
- s = Length along airfoil surface, measured aft from leading edge
- V = Velocity
- x = Length along airfoil chord, measured aft from leading edge
- α = Airfoil angle of attack, radians, unless otherwise noted
- α_r = Rotor blade-element angle of attack, measured from line of zero lift, radians
- Δ = Increment

δ^* = Boundary-layer displacement thickness

ν = Kinematic viscosity

Subscripts

A = Average

C = Compressible

i = Incompressible

L = Local

MIN = Minimum

O = Free-stream

OL = Zero lift

R = Rough

S = Smooth

x = Length along airfoil chord

α = Due to angle of attack